

Monopole and Dirac string Dynamics in Spin Ice

L. D. C. Jaubert¹ and P. C. W. Holdsworth¹

¹*Université de Lyon, Laboratoire de Physique, École Normale Supérieure de Lyon,
46 Allée d'Italie, 69364 Lyon Cedex 07, France.*

Magnetic monopoles have eluded experimental detection since their prediction nearly a century ago by Dirac¹. Recently it has been shown that classical analogues of these enigmatic particles occur as excitations out of the topological ground state of a model magnetic system, dipolar spin ice². These quasi-particle excitations do not lead to a modification of Maxwell's equations, but they do interact via Coulombs law and they are of magnetic origin. In this paper we present an experimentally measurable signature of monopole dynamics and show that magnetic relaxation measurements in spin ice materials can be interpreted entirely in terms of their diffusive motion on a diamond lattice in the grand canonical ensemble. The monopole trajectories are constrained to lie on a network of Dirac strings filling the quasi-particle vacuum. We find quantitative agreement between the time scales for relaxation in the Dirac string network and the magnetic relaxation data for the spin ice material $Dy_2Ti_2O_7$ [3]. In the presence of a magnetic field the topology of the network prevents charge flow in the steady state, but transient monopole currents do occur, as well as monopole density gradients near the surface of an open system.

Spin ice systems^{4,5,6} such as $Dy_2Ti_2O_7$ and $Ho_2Ti_2O_7$, can be described by a corner sharing network of tetrahedra forming a pyrochlore lattice of localized magnetic moments, as shown in figure 1a. The pairwise interaction is made up of both exchange and dipolar terms

$$\mathcal{H} = J\mu^2 \sum_{\langle i,j \rangle} \mathbf{S}_i \cdot \mathbf{S}_j + D\mu^2 \sum_{\langle i,j \rangle} \left[\frac{\mathbf{S}_i \cdot \mathbf{S}_j}{|\mathbf{r}_{ij}|^3} - \frac{3(\mathbf{S}_i \cdot \mathbf{r}_{ij})(\mathbf{S}_j \cdot \mathbf{r}_{ij})}{|\mathbf{r}_{ij}|^5} \right] \quad (1)$$

where the rare earth ions carry a moment of ten Bohr magnetons, $\mu = 10\mu_B$ and where \mathbf{S}_i is a spin of unit length. The coupling constants are on the 1 K energy scale; for example for $Dy_2Ti_2O_7$ $|J|m^2 \approx 3.72 K$ and $Dm^2 \approx 1.41 K$ [7]. These energy scales are 100 times smaller than the crystal field terms⁸ that confine the spins along the axis joining the centres of two adjoining tetrahedra. As a result, on the 1 K energy scale the moments behave as Ising spins pointing in one of two directions along this line, while the centres of the tetrahedra form a diamond structure (see figure 1). Remarkably, within this Ising description the long ranged dipole interactions are almost perfectly screened^{7,9} at low temperature down to 1K, with the result that the low energy properties are almost identical to those of an effective nearest neighbour model with ferromagnetic interactions of strength $J_{eff} = (5D - J)m^2/3$. This is equivalent to Pauling's model for proton disorder in the cubic phase of ice¹⁰, which has extensive ground state entropy and violates the third law of thermodynamics⁶. It successfully reproduces the thermodynamic behaviour of both ice¹¹ and spin ice¹² and describes the microscopic properties of the latter to a good approximation. The extensive set of spin ice states satisfy the Bernal - Fowler ice rules¹³; a 3d analogue of the 6 vertex model with topological constraint consisting of two spins pointing into and two out of each tetrahedron (2 in - 2 out), as shown in figure 1a. Flipping one spin breaks the constraint leaving neighbouring tetrahedra with 3 in - 1 out and with 3 out - 1 in, which constitute a pair of topological defects (see Fig. 1a). Within the nearest neighbour model, creation of the defect pair costs energy $4J_{eff}$, while further spin flips can move the defects at zero energy cost. It has recently been shown² that including the full dipolar Hamiltonian (1) leads to an effective Coulombic interaction between the topological defects separated by distance r , $\mu_0 q_i q_j / 4\pi r$, where μ_0 is the permeability of free space, $q_i = \pm q = \pm 2m/a$, and a is the distance between two vertices of the diamond lattice; that is, to a Coulomb gas of magnetic monopoles. Standard electromagnetic theory does allow for such excitations¹⁴, which correspond to divergences in the magnetic intensity, \mathbf{H} , or magnetic moment \mathbf{M} , rather than in the magnetic induction: $\nabla \cdot \mathbf{B} = \nabla \cdot (\mathbf{H} + \mathbf{M}) = 0$. On all length scales above the atomic scale, a 3 in - 1 out defect appears to be a local sink in the magnetic moment and therefore as a source of field lines in \mathbf{H} . It can lower its energy by moving in the direction of an external field and therefore carries a positive magnetic charge¹⁵. A two dimensional equivalent may exist in artificial spin ice, constituting arrays of nanoscale magnets^{16,17}. But what is remarkable about

real spin ice is that it allows for the deconfinement of these effective magnetic charges so that they occur in the bulk of the material on all scales, rather than just at the surfaces within a coarse grained description¹⁴.

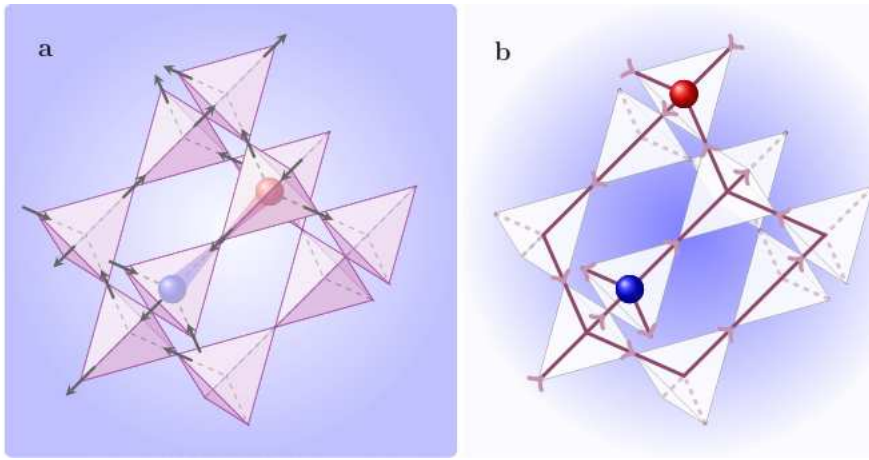


FIG. 1: The magnetic ions (Ho or Dy) lie on the sites of the pyrochlore lattice formed by a corner-sharing ensemble of tetrahedra. The Ising like spins are constrained to the bonds of the dual (diamond) lattice (dashed lines). For a single tetrahedron, configurations respecting the ice rules (2 in - 2 out) are energetically favoured while local topological excitations 3 in - 1 out or 3 out - 1 in correspond to magnetic monopoles with positive (blue sphere) or negative (red sphere) charges respectively. b) The dual (diamond) lattice provides the skeleton for the network of Dirac strings with the position of the monopole restricted to the vertices. The orientation of the Dirac strings shows the direction of the local field lines in \mathbf{H} . The positive and negative charges appear respectively as sources and sinks of \mathbf{H} .

Given the accessibility of these magnetic quasi-particles, the development of an experimental signature is of vital importance and interest. The “Stanford” superconducting coil experiment¹⁸ could in principle detect the passage of a single magnetic quasi-particle, but this seems highly unlikely given that the estimated magnetic charge is four orders of magnitude smaller than that of a Dirac monopole² and that the charges have diffusive, rather than Newtonian dynamics. A more promising starting point is therefore to look for a monopole signal from magnetic relaxation of a macroscopic sample^{3,8,19}. The general dynamic behaviour of spin ice is illustrated in figure 2 by the magnetic relaxation time, as a function of temperature for $Dy_2Ti_2O_7$ ^[3], taken from bulk susceptibility measurements. On cooling, the time scale increases below $18K$, entering a quasi-plateau region below $12K$, before experiencing a sharp upturn below $2K$. The high (h - above $12K$) and low (ℓ) temperature regimes are respectively associated with thermally activated, and quantum tunnelling processes⁸ and are a manifestation of the energy scales discussed in equation (1) : below $12K$ the spins are Ising like and the configuration evolves by quantum tunnelling through the crystal field barrier, while above this temperature higher crystal field levels are populated and the time scale drops dramatically. The quantum tunnelling plateau regime can therefore be well represented by an Ising system with stochastic single spin dynamics and hence should be dominated by the propagation of monopole objects. This is illustrated, in a first approximation, by comparing the data with an Arrhenius law $\tau = \tau_0 \exp(2J_{eff}/k_B T)$, as shown in figure 2 (inset). The time scale; τ_0 , is fixed by equating with the experimental time at $4K$ with $J_{eff} = 1.11 K$, the value estimated for $Dy_2Ti_2O_7$ ^[7]. $2J_{eff}$ is the energy cost of a single, deconfined topological defect in the nearest neighbour approximation for $Dy_2Ti_2O_7$ and is half that for a single spin flip. The calculation fits the data over the plateau region, where one expects a high defect concentration, and gives surprisingly good qualitative agreement at lower temperature, as the concentration decreases. The good fit in the paramagnetic plateau region equates with the microscopic tunnelling time, making the fit at low temperature a stringent test for both the Arrhenius process and the value of the barrier height. This test therefore already provides very strong evidence for the fractionalization of magnetic charge² and the free diffusion of unconfined particles. However, the Arrhenius law and hence the nearest neighbour model ultimately fails, underestimating the time scale at low temperature. The role of the missing Coulomb interaction is therefore clear : although non-confining it will lead to locally bound pairs of particles, considerably slowing down diffusion and

increasing the time scale.

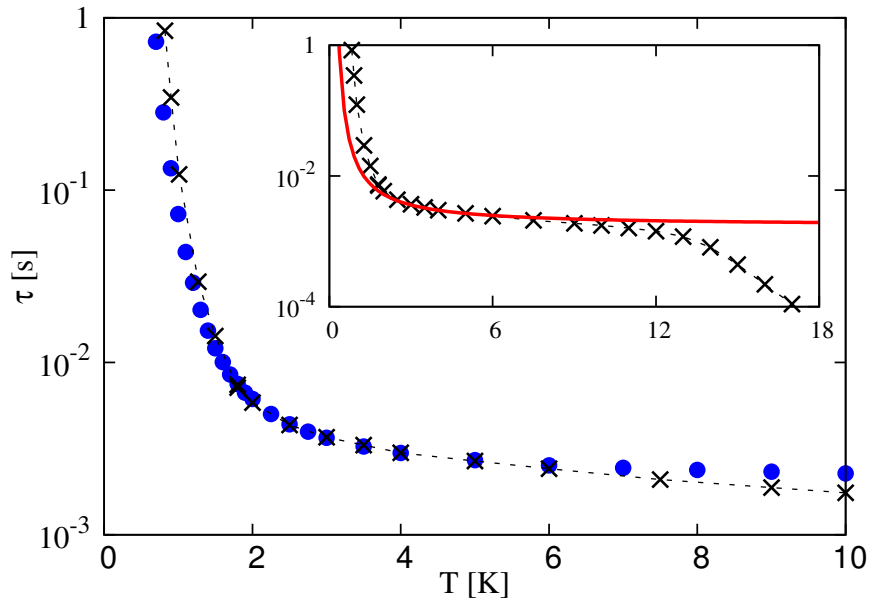


FIG. 2: Both inset and main figures show the relaxation time scale, τ , in seconds as a function of temperature. The experimental data (black cross) are from Snyder & al.³. Inset : The Arrhenius law (red line) for the nearest neighbour model reproduces the experimental data in the plateau region but is not sufficient to explain in detail the sharp slowing down of the dynamics at low temperature. Main : Relaxation time scale of the Dirac string network driven by Metropolis dynamics of magnetic monopoles (blue dot). The simulation describes the experimental data quantitatively both in the plateau and low temperature regions. The temperature scale is fixed without any free parameters.

We have tested this idea by directly simulating a Coulomb gas of magnetically charged particles (monopoles), in the grand canonical ensemble, occupying the sites of the diamond lattice. The magnetic charge is taken as $q_i = \pm q$ while the chemical potential is the difference between the Coulomb energy gained by creating a pair of neighbouring magnetic monopoles and that required to produce a pair of topological defects in the dipolar spin ice model : it is thus not a free parameter. As the Coulomb interaction is long ranged, we treat a finite system of size L using the Ewald summation method^{20,21}. The monopoles hop between nearest neighbour sites via the Metropolis Monte Carlo algorithm, giving diffusive dynamics, but with a further local constraint : in the spin model a 3 in - 1 out topological defect can move at low energy cost by flipping one of the three in spins, the direction of the out spin being barred by an energy barrier of $8J_{eff}$. An isolated monopole can therefore hop to 3 out of 4 of its nearest neighbour sites only, dictated by an oriented network of constrained trajectories similar to the ensemble of classical “Dirac strings”² of overturned dipoles¹⁴. The positively charged monopoles move in one sense along the network while the negative charges move in the opposite direction (see Fig. 1b). The network is dynamically re-arranged through the evolution of the monopole configuration. The vacuum for monopoles in spin ice thus has an internal structure ; the Dirac strings which, in the absence of monopoles, satisfy the ice rules at each vertex of the diamond lattice. This structure is manifest in the dynamics and influences the resulting time scales. In fact the characteristic time scale that we compare with experiment comes from the evolution of the network of Dirac strings rather than from the monopoles themselves. Indeed, the monopole autocorrelation time, as extracted from the monopole density - density correlation function²² turns out to be small for this range of temperature. We locally define the string network by an integer $\sigma = \pm 1$, giving the local orientation of the Dirac string along each bond of the diamond lattice and define the autocorrelation function

$$C(t) = \frac{1}{N} \sum_i \sigma_i(t) \sigma_i(0), \quad (2)$$

where t is the Metropolis time and N is the number of bonds. For the initial conditions we take an ordered network with no monopoles, which we let evolve at temperature T until an equilibrium

configuration is attained. This defines $t = 0$. $C(t)$ decays almost exponentially, with characteristic time, τ , that varies with temperature. To avoid initial transient effects we define τ such that $C(\tau) = 0.8$. The time is re-set to zero when $C(t)$ decays beyond 0.01 and the process is repeated many times to give the configurationally averaged decay time. In figure 2 we compare our data with the experimental data of ref.³ from zero to 10K. The Metropolis time is again scaled to the experimental time at 4K and there is again no scale factor on the temperature axis. There is excellent quantitative agreement between the experimental and numerical data, showing clearly that the experimental relaxation is due to the creation and proliferation of quasi-particle excitations that resemble classical monopoles in the magnetic intensity \mathbf{H} . Further, the improvement in the results compared with figure 2 (inset), emphasizes the importance of the Coulomb interaction between the particles in the temperature dependence of the relaxation time scales. As the temperature increases, towards the end of the plateau region, a small systematic difference occurs. This is because the spin system can access states with all spins in or out at finite energy cost, while this state corresponds to two like charges superimposed on the same site, which is excluded by the Coulomb interaction.

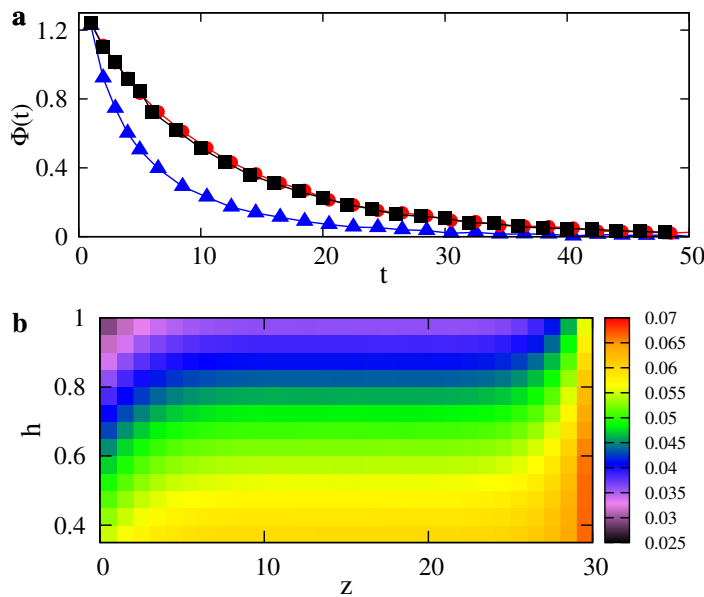


FIG. 3: An external field is applied at $t = 0$ along the [100] cubic direction. We display the transient flux of positive charges, Φ , passing through a plane perpendicular to the field, as a function of Metropolis time, t . The simulations are obtained using the nearest neighbour spin ice model with periodic boundary conditions (black square) and open boundaries; the flux is then computed at the surface (blue triangle) and in the bulk (red dot). The current is always zero in the steady state. b) Transient currents lead to a surface charge build up. The figure shows the density of positive defects (3 in - 1 out) in the horizontal plane as a function of the vertical axis z along the field and for different values of the field, h in units of $k_B T / m \mu_0$.

Finally we consider the response of monopoles to an external magnetic field, h , placed along one of the [100] directions. Applying such a field to a system with periodic boundaries, one might expect the development of a monopole current in the steady state¹⁵. This is not the case, at least for the nearest neighbour model, where we find that a transient current decays rapidly to zero (see Fig. 3a). The passage of a positive charge in the direction of the field re-organises the network of strings, leaving a wake behind it that can be followed either by a negative charge, or by a positive one moving against the field, with the result that the current stops. This is a dynamic rather than static effect and is not related to confinement of monopole pairs by the background magnetization². Reducing the temperature at finite field, the magnetization saturates around a critical temperature; a vestige of the Kasteleyn transition²³, which is unique to topologically constrained systems. Confinement occurs here, as the Zeeman energy out weighs the entropy gain of free monopoles. The transient currents suggest the development of charge separation in an open system. This is indeed the case despite the fact that monopole numbers are not conserved at open boundaries. In figure 3b we show the profile of positive charge density across a sample of size L , with open boundaries, for varying fields. There is a clear build up of charge over a band of 4–5

lattice spacings, although including long range interactions may lead to a quantitative change in this value. As the ratio T/h and the monopole density go to zero the band narrows and the system forms a conventional layer of magnetic surface charge as one expects for any magnetically ordered system¹⁴. In the absence of topological defects the magnetization is conserved from one layer to another, so that a charge density profile manifests itself as a magnetization profile. The data here suggest charge build up in a layer several nanometres thick, making it in principle a measurable effect.

-
- ¹ Dirac, P. A. M. Quantised singularities in the electromagnetic field. *Proc. R. Soc. A* **133**, 60-72 (1931).
 - ² Castelnovo, C., Moessner, R. & Sondhi S. Magnetic monopoles in spin ice. *Nature* **451**, 42-45 (2008).
 - ³ Snyder, J. et al. Low-temperature spin freezing in the $Dy_2Ti_2O_7$ spin ice. *Phys. Rev. B* **69**, 064414 (2004).
 - ⁴ Harris, M. J., Bramwell, S. T., McMorro, D. F., Zeiske, T. & Godfrey, K. W. Geometrical Frustration in the Ferromagnetic Pyrochlore $Ho_2Ti_2O_7$. *Phys. Rev. Lett.* **79**, 2554-2557 (1997).
 - ⁵ Bramwell, S. T. & Gingras, M. J. P. Spin Ice State in Frustrated Magnetic Pyrochlore Materials. *Science* **294**, 1495-1501 (2001).
 - ⁶ Bramwell, S. T., Gingras, M. J. P. & Holdsworth, P. C. W. *Frustrated Spin Systems*, Ch. 7 (H. T. Diep, World Scientific, Singapore, 2004).
 - ⁷ den Hertog, B. C. & Gingras, M. J. P. Dipolar Interactions and Origin of Spin Ice in Ising Pyrochlore Magnets. *Phys. Rev. Lett.* **84**, 3430-3433 (2000).
 - ⁸ Ehlers, G. et al. Dynamical crossover in 'hot' spin ice. *J. Phys. : Condens. Matter* **15**, L9-L15 (2003).
 - ⁹ Isakov, S. V., Moessner, R. & Sondhi, S. Why spin ice obeys the ice rules. *Phys. Rev. Lett.* **95**, 217201 (2005).
 - ¹⁰ Pauling, L. The Structure and Entropy of Ice and of Other Crystals with Some Randomness of Atomic Arrangement. *J. Am. Chem. Soc.* **57**, 2680-2684 (1935).
 - ¹¹ Giaouque, W. F. & Stout, J. W. The entropy of water and the third law of thermodynamics. The heat capacity of ice from 15 to 273 K. *J. Am. Chem. Soc.* **58**, 1144-1150 (1936).
 - ¹² Ramirez, A. P., Hayashi, A., Cava, R. J., Siddharthan, R. & Shastry, B. S. Zero-point entropy in spin ice. *Nature* **399**, 333-335 (1999).
 - ¹³ Bernal, J. D. & Fowler, R. H. A theory of water and ionic solution, with particular reference to hydrogen and hydroxyl ions. *J. Chem. Phys.* **1**, 515-548 (1933).
 - ¹⁴ Jackson, J. D. *Classical Electrodynamics* Ch. 6.11-6.12 (Wiley, New-York, 1999).
 - ¹⁵ Ryzhkin, I. A. Magnetic relaxation in rare-earth oxide pyrochlores. *J. Exp. Theor. Phys.* **101**, 481-486 (2005).
 - ¹⁶ Wang, R. F. et al. Artificial spin ice in a geometrically frustrated lattice of nanoscale ferromagnetic islands. *Nature* **439**, 303-306 (2006).
 - ¹⁷ MI, L. A. S. et al. Magnetic monopole and string excitations in a two-dimensional spin ice. Preprint at <http://arXiv.org/abs/0809.2105v1>.
 - ¹⁸ Cabrera, B. First results from a superconductive detector for moving magnetic monopoles. *Phys. Rev. Lett.* **48**, 1378-1381 (1982).
 - ¹⁹ Matsuhira, K., Hinatsu, Y., Tenya, K. & Sakakibara, T. Low temperature magnetic properties of frustrated pyrochlore ferromagnets $Ho_2Sn_2O_7$ and $Ho_2Ti_2O_7$. *J. Phys. : Condens. Matter* **12**, L649-L656 (2000).
 - ²⁰ de Leeuw, S. W., Perram, J. W. & Smith, E. R. Simulation of electrostatic systems in periodic boundary conditions. I. Lattice sums and dielectric constants. *Proc. R. Soc. London A* **373**, 27-56 (1980).
 - ²¹ Frenkel, D. and Smit, B. *Understanding Molecular Simulation : from Algorithms to Applications* Ch. 12.1 (Academic Press, San Diego, London, 2002).
 - ²² See for example, Barrat, J.-L. and Hansen, J.-P. *Basic Concepts for Simple Liquids* Ch. 11 (CUP, Cambridge, 2003).
 - ²³ Jaubert, L. D. C., Chalker, J. T., Holdsworth, P. C. W. & Moessner, R. A three dimensional Kasteleyn transition : spin ice in a [100] field. *Phys. Rev. Lett.* **100**, 067207 (2008).

Acknowledgements We thank S.T. Bramwell, C. Castelnovo, M. Clusel, M.J.P. Gingras and R. Melko for useful discussions and P. Schiffer for providing the data from reference ^[3].

Author Information Correspondence should be addressed to L.J. (e-mail : ludovic.jaubert@ens-lyon.org).